R. GIOVANELLI

Relativistic Electron Motion in FEL-Like Fields Taking Retarded Interactions Into Account.

Estratto da
Il Nuovo Cimento - Vol. 15 D, N. 1 - Gennaio 1993 - pp. 23-38

EDITRICE
COMPOSITORI
BOLOGNA
1993

IL NUOVO CIMENTO Vol. 15 D, N. 1 Gennaio 1993

Relativistic Electron Motion in FEL-Like Fields Taking Retarded Interactions Into Account.

R. Giovanelli
Facoltà di Scienze dell'Università - Parma

(ricevuto il 23 Settembre 1992; approvato l'1 Ottobre 1992)

Summary. — The interaction of two charged particles both with each other (via Lienard-Wiechert retarded potentials) and with the wiggler field of an FEL structure, along which they are launched, is computed by means of the numerical integration of the relativistic motion equations, taking also an incoming laser wave into account. The bunching effect characterizing the collective behaviour of an electron beam in FEL-like fields is simulated by assuming one of the particles to be a suitable macrocharge.

PACS 42.55.Tb – Free electron lasers.
PACS 52.65 – Plasma simulation.

1. – Introduction.

As is well known, the relativistic Hamiltonian [1] of a system of charged particles interacting with each other and with external electromagnetic fields may be written only in the limiting case of a single particle in external fields and, because of the impossibility of considering retarded interactions in the case of a system of particles in non-relativistic motion with respect to their centre of mass (which is allowed, however, to be endowed with a relativistic velocity). Breit's Hamiltonian (derived from Darwin's Lagrangian [2, 3]), is the most practical model currently employed for atomic systems.

Although some progress was indeed performed [2, 4], the very possibility of applying relativity (and even quantum mechanics) is strongly limited, as shown in any textbook of relativistic electrodynamics [3], the main difficulty consisting in the non–Lorentz-invariant character of the interaction terms, based on simultaneity, which is not relativistically invariant [5].

A quite easier task is the study of the so-called undulators, where high-energy electrons interact with an undulated transverse magnetic field. No external electric field is present and the electric interaction of charged particles with each other (*i.e.* collective phenomenon) is negligible. In these conditions, the relativistic motion equation of a charge may be analitically integrated. Complete solutions of the spectral emission from a single particle were obtained in ref. [6] even for direction diverging

from the undulator axis. This treatment, however, is of limited interest in cases when collective phenomena in an FEL structure must be taken into account.

Current papers describing the physics of FEL in Raman regime (*i.e.* for high beam currents) employ the Hamiltonian approach [7], and must therefore remain limited to non-relativistic motions in the centre of mass system, thus requiring, for instance, an external magnetic field low enough to deflect electrons with non-relativistic transversal velocities. Renouncing here to tackle the heavy problem of the many-particle relativistic Hamiltonian, we shall describe the electron motion in an FEL geometry by means of a model based on non-Hamiltonian relativistic dynamics, considering both radiation damping and retarded interactions and making use, therefore, of a treatment acceptable from the point of view of causality. Other models proposed for 3-D simulations of FEL laser physics [8] neglect retardation in particle interactions.

The techniques employed in the numerical simulations of free-electron lasers are summarized in [9], where also the time-dependent simulations are included; but the effects due to fast transient radiation interaction between charges are masked by the use of Fourier transforms, applied to physical models where the electromagnetic-field amplitude is supposed periodical with a poor frequency spectrum. Our main aim is to consider here, by means of a numerical approach, the evolution of a system composed of two particles (one of which may be a macroparticle) interacting both with each other and with external FEL-like fields. While such a model turns out to give information of quite general interest on FEL dynamics, the extension to a system of many electrons, taking mutual perturbations into account, does not appear to be of practical interest for numerical applications. In sect. 2 of the present paper, the mathematical formulation of the particle motion and field radiation equations is presented. In sect. 3, the conditions to obtain simplified equations are deduced. In sect. 4, numerical results are given for two charged particles interacting through their electromagnetic radiation. The description of the numerical method employed here, and of partially analytical equivalent approach are deferred, respectively, to appendices A and B.

2. – Physical model—electron motion and radiation fields.

We assume a coordinate system where $\hat{x}$ is the wiggler axis along which the particle is launched, and $\hat{z}$ the direction of the wiggler magnetic field (fig. 1).

The Lorentz equations for the electron motion may be written (in Gaussian units) in the form

$$\frac{\mathrm{d}\underline{p}}{\mathrm{d}t} = e\left[\underline{E} + \frac{\underline{p}\times\underline{B}}{mc\gamma}\right] = \underline{F}, \tag{2.1}$$

$$\underline{v} = \frac{\mathrm{d}\underline{x}}{\mathrm{d}t} = \frac{\underline{p}}{m\gamma}, \tag{2.2}$$

$$\frac{\mathrm{d}\gamma}{\mathrm{d}t} = \frac{e}{m^2c^2\gamma}\underline{p}\cdot\underline{E}, \tag{2.3}$$

where $\gamma = [1 - (v/c)^2]^{-1/2}$ and m is the electron rest mass.

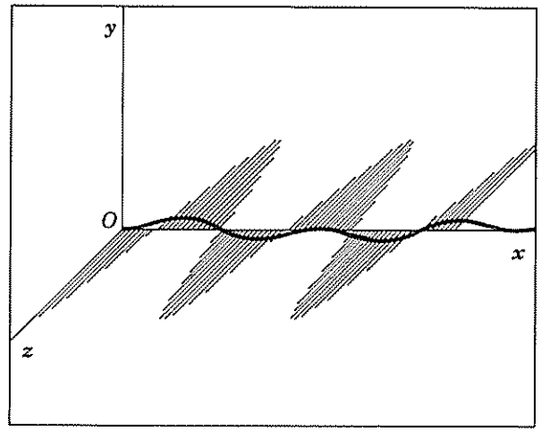

Fig. 1. – FEL geometry. The undulated thick line represents a particle orbit. The wiggler magnetic field is represented by the shaded areas.

The force $\underline{F}$ includes both the external and mutual forces computed from the sources at the previous time $t' = t - R/c$.

The electric and magnetic field, respectively generated at the point $P(\underline{x}, t)$ by a particle of charge «e» placed at $P'(\underline{x}', t')$, may be written [10] in the form

$$\underline{E}(\underline{x}, t) = e\frac{(\hat{n} - \underline{\beta})(1-\beta^2)}{\chi^3 R^2} + \frac{e}{c\chi^3 R}[\hat{n}\times\{(\hat{n} - \underline{\beta})\times\dot{\underline{\beta}}\}], \tag{2.4}$$

$$\underline{B}(\underline{x}, t) = \hat{n}\times\underline{E}(\underline{x}, t), \tag{2.5}$$

where $\underline{\beta} = \underline{v}/c$, $\chi = (1 - \hat{n}\cdot\underline{\beta})$, $\underline{R} = (\underline{x} - \underline{R}(t'))$, $\dot{\underline{\beta}} = \mathrm{d}\underline{\beta}/\mathrm{d}t$ and $\hat{n} = \underline{R}/R$ is the unit vector along $\underline{R} = (\underline{x}' - \underline{x})$. The geometry is represented in fig. 2. The fields $\underline{E}$ and $\underline{F}$ are represented in fig. 3.

The first term of eq. (2.4), generally called «velocity field», is independent of the acceleration $\dot{\underline{\beta}}$, while the second one, called «acceleration field», depends linearly on $\dot{\underline{\beta}}$.

The velocity fields are conservative, and fall off as R^{-2}, whereas the acceleration fields have a typically radiative nature with vectors transverse to $\underline{R}$ and varying as R^{-1}.

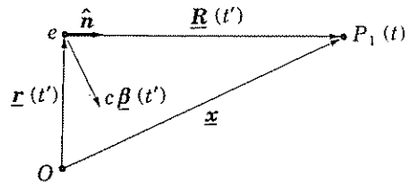

Fig. 2. – The point charge (e) at the position $\underline{r}(t')$, with velocity $c\underline{\beta}(t')$ has a distance $\underline{R}(t')$ from the observation point $P_1(x, t)$. The direction $\hat{n}(t') = \underline{R}/R$ changes with the previous position of the point charge.

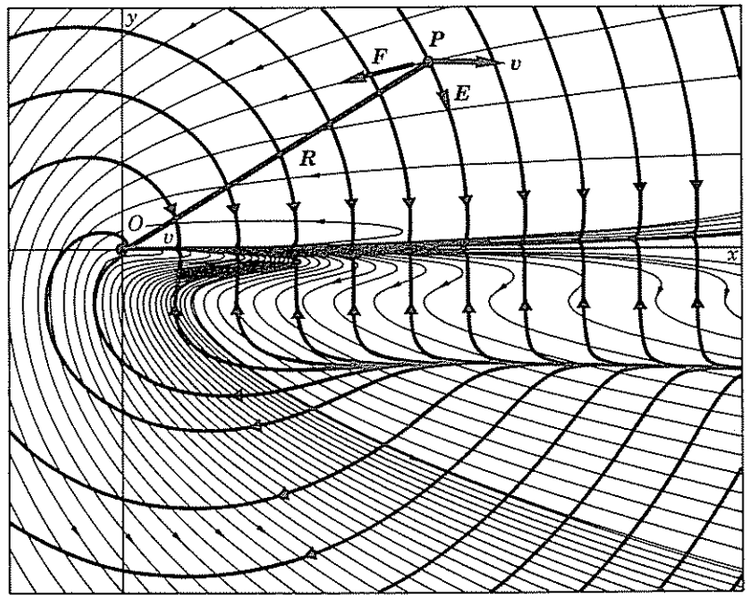

Fig. 3. – In all the points P of the plane (x, y) a charge $-e$, with velocity $\underline{v} = c\underline{\beta}(t')$ parallel to the $\hat{x}$-axis, has a distance $\underline{R}(t')$ from the origin O where the source point charge, also equal to $-e$, is placed. Thin lines represent the force $\underline{F} = -e(\underline{E} + \underline{\beta} \times \underline{B})$, where $\underline{E}$ and $\underline{B}$ are the fields generated by the charge placed in O. Thick lines represent the field of the electric component of $\underline{F}$. Theparticle moves in a transverse magnetic field $B_z = 5000$ gauss.

3. – Particular radiation cases.

a) By introducing, as shown in fig. 4*a*) a vector $\underline{r}(t')$ representing the position of the emitting charge and the unit vector $\hat{n}$ along the fixed position vector $\underline{x}$ of the observing point P, it may be shown that, in the particular case of the fields observed at large distance from an emitting electron (and also when the vector $\underline{R}(t')$—see fig. 4*b*)—is almost parallel to $\hat{n}$), the distance $R(t')$ between the emitting and the

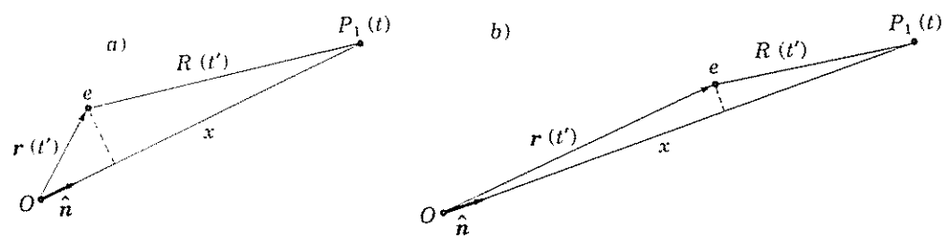

Fig. 4. – *a*) The observation point P_1 is assumed to be very far from the region where the radiation occurs. We may approximate $R(t') \cong x - \hat{n} \cdot \underline{r}(t')$, where x is the distance between the origin O and the observation point P_1, and $\underline{r}(t')$ is the position of the radiation charge relative to O. The direction $\hat{n}$ of $\overline{OP}$ is fixed in space. *b*) When $|\underline{r}|$ is comparable to R but $\underline{r}$ and $\hat{n}$ are almost collinear we may again approximate $R(t') \cong x - \hat{n} \cdot \underline{r}(t)'$ as in *a*).

observing point may be approximated (fig. 4*a*)) as

$$R(t') \cong x - \hat{n} \cdot \underline{r}(t'), \tag{3.1}$$

so that the energy radiated per unit solid angle and per unit frequency interval, $\mathrm{d}I(\omega, \hat{n})/\mathrm{d}\Omega$ may be given in a simplified form in terms of an integral over the particle trajectory [3]

$$\frac{\mathrm{d}I(\omega, \hat{n})}{\mathrm{d}\Omega} = \frac{e^2\omega^2}{4\pi^2 c} \left| \int_{-\infty}^{\infty} \mathrm{d}t' \, \hat{n} \times [\hat{n} \times \underline{\beta}(\underline{r}(t'))] \exp[i\omega[t' - (\hat{n} \cdot \underline{r}(t'))/c]] \right|^2 . \tag{3.2}$$

Although not explicitly dependent on $\dot{\underline{\beta}}$, such an expression may be shown to vanish when $\dot{\underline{\beta}} = 0$. An important feature of eq. (3.2) is seen to be its independence from time.

This approximation, however, cannot be accepted when the field is evaluated close to the emitting charge, far from the direction of motion (the beam axis). We represent in fig. 4*a*) and *b*) two cases differing only for the choice of the coordinates origin O.

The first one is that, usually considered, characterized by an observation point P very far from the radiation region; the second one is the typical case of an FEL, where the size of the source (or the order of some meters) is not small in comparison with the distance from the observation point.

The integral (3.2), performed along the particle trajectory in terms of the laboratory time, describes the final radiation spectrum, thus requiring the previous knowledge of the trajectory itself: eq. (3.2) may therefore be employed only in near-stationary conditions and does not supply the phases of radiation harmonics.

Equation (3.2) does not allow therefore the analysis of instability phenomena due to the radiative-particle interactions.

In the resonant case of the coherent emission of a beam consisting of a series of bunches spaced at a distance equal to the wavelength λ_L of the emitted radiation, the knowledge of the radiative phase is not necessary, and eq. (3.2) gives the required information about the harmonic amplitudes. In transient phenomena, however, eq. (3.2) is not able to give the phase of the emitted radiation and cannot correctly compose the harmonic amplitudes.

In general, therefore, eqs. (2.4) and (2.5) must be employed in their complete form. We can verify the limits of the approximation (3.2) considering the simplified case of two interacting charges in FEL geometry, where all the electrons move along the FEL axis $\hat{x}$ with a straight average trajectory, oscillating back and forth transverse to it with amplitude $y_{\max} = \sqrt{2} \cdot a_W/(k_W \gamma)$. Let P_0 be the position at the time t of a charge moving along $\hat{x}$ with the mean velocity $V = \beta c$ (fig. 5), and P_1 the position of the other charge assumed to move with the same velocity, at the same time t. Let us assume the position of the first particle as the origin of a suitable reference frame, where the position of the second particle is individuated in polar form by the distance $d\,(= \overline{P_0 P_1})$ and by the angle α between the vector $\overline{P_0 P_1}$ and $-\hat{x}$. Let us define the position P_0' (at the previous time t') of the first charge such that its radiation hits the other particle at the position P_1 at the time t, under the assumption that both average trajectories are rectilinear.

The position of P_0' shall be defined by the distance R between the radiation point

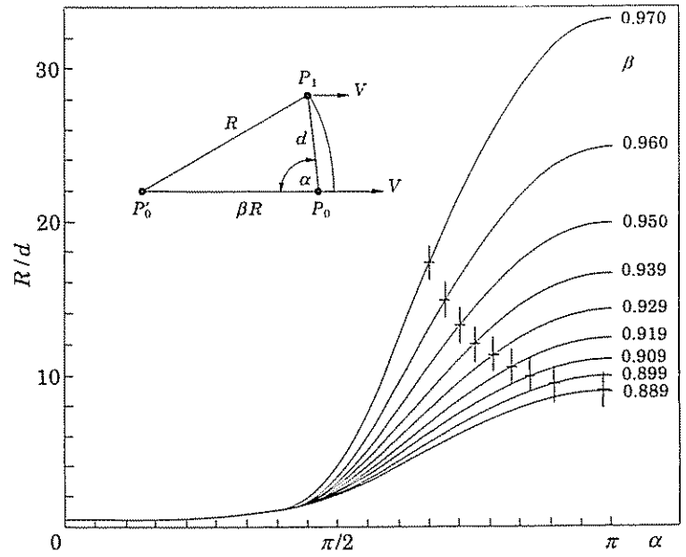

Fig. 5. – Plot *vs.* α of the distance R at the previous time $t' = t - R/c$ for different values of the average velocity $V = \beta c$. Above the indicated cross, each diagram satisfies condition (3.1).

P_0' and the receiving point P_1 obtained from the relation

$$R^2 = d^2 + \beta^2 R^2 - 2d\beta R \cos\alpha ,$$

that leads to

$$\frac{R}{d} = \frac{-\beta\cos\alpha + [1 - \beta^2 \sin^2\alpha]^{1/2}}{1 - \beta^2} . \tag{3.3}$$

As shown in fig. 5, the distance R turns out to be not much larger than d for $\alpha \leqslant \pi/2$. If we assume for d the values λ_L, the approximation (3.1) shall require that: $R/\lambda_L \gg y_{max}/\lambda_L$. For an FEL with $B_W = 5\,000$ Gauss and $\lambda_W = 2$ cm, condition (3.2) is satisfied only on the side of each diagram of fig. 5 above the indicated cross.

b) If the electromagnetic (optical) fields are described by the vector potential $\underline{A}$ [3], we may write, disregarding the electric potential Φ, the wave equation

$$\nabla^2 \underline{A} - \frac{1}{c^2}\frac{\partial^2 \underline{A}}{\partial t^2} = -\frac{4\pi}{c}\underline{J}_t , \tag{3.4}$$

where $\underline{J}_t$ is the electron beam transverse-current density. Ignoring second derivatives and squares of first derivatives of the function $\underline{A}$ (supposed a slowly varying function [7]), a first-order partial differential equation is obtained from eq. (3.4), that leads to solutions which do not depend on the previous time t'. No transient disturbance can therefore be described.

In both cases, described, respectively, in *a*) and *b*) it is seen, in conclusion,

that disregarding the time-dependence of the radiated fields makes it impossible to detect any transient and/or localized phenomenon.

4. – Numerical results for two interacting charged particles.

The radiative interaction between the charges of a beam, leading to a trajectory modification, affects, since the very beginning, the acceleration and therefore the emission of irradiated charges.

Let us consider, for the moment, the radiating part alone of the fields (2.4) and (2.5). As is well known, the radiation is mainly contained in a cone of aperture $1/\gamma$. Let two charges 1 and 2 (charge 2 being ahead with respect to charge 1) travel along the $\tilde{x}$-axis with velocity $\underline{\beta}c$, at mutual distance $\beta\lambda_L$, where $\lambda_L = \lambda_W (1 + a_W^2)/2\gamma^2$ is the radiation FEL wavelength, λ_W the FEL wiggler wavelength, $a_W = eB_W/(\sqrt{2}k_W mc^2)$ the interaction strength due to the wiggler magnetic field B_W and $k_W = 2\cdot\pi/\lambda_W$ is the wavenumber corresponding to the wiggler wavelength λ_W. In these conditions, resonance is possible with a radiation (with wavelength λ_L) propagation along $\tilde{x}$. As the backward charge radiation is negligible (backward electric field radiated by 2 to 1 is: $\underline{E}^{(2)}_{rad/back} \cong -\tilde{y}e\cdot\dot{\beta}^{(2)}/(2c\lambda_L)$), only particle 2 is affected by the radiated fields. If particle 2 is reached by the radiation (emitted by 1) at $t = 0$, such a radiation must be sent by particle 1 at $t = -\lambda_W/c$. Both radiating particles are taken to be in a wiggler position where the magnetic field $\underline{B}_W = \tilde{z}\cdot B_W \sin(k_W x)$ is maximum.

The electric field radiated by 1 is given by the radiative part of (2.4):

$$\underline{E}^{(1)}_{rad} \cong -\tilde{y}\frac{e\dot{\beta}^{(1)}\cdot 4\cdot\gamma^4}{c\lambda_W} ,$$

where the acceleration $\underline{\beta}^{(1)}$ is given by

$$\dot{\underline{\beta}}^{(1)} = -\tilde{y}e\beta B_W/(m\gamma c) .$$

The corresponding magnetic field is obviously

$$\underline{B}^{(1)}_{rad} = \tilde{z}\underline{E}^{(1)}_{rad} .$$

The acceleration of particle 2 is given by

$$\dot{\underline{\beta}}^{(2)} = \dot{\underline{\beta}}^{(1)} + \tilde{y}\frac{e^3 B_W\cdot 4\cdot\gamma^2}{m^2c^3\lambda_W} ,$$

where the term added to $\dot{\underline{\beta}}^{(1)}$ is determined by the fields $\underline{E}^{(1)}_{rad}$ and $\underline{B}^{(1)}_{rad}$. It must be observed that this correction is generally small with respect to $\dot{\underline{\beta}}^{(1)}_{rad}$ but of opposite sign.

The radiative interaction acting all along the entire trajectory of particle 2 is the actual cause of the amplification process.

The total fields acting along the trajectories of mutually interacting electrons are found by adding to the radiation fields of all the electrons of the beam (computed by means of the Lienard-Wiechert retarded potentials of the individual electrons) the incoming external laser fields [11].

The modulating external laser fields, with their transverse components, produce a longitudinal ponderomotive force [12], resulting from the beating of the laser fields

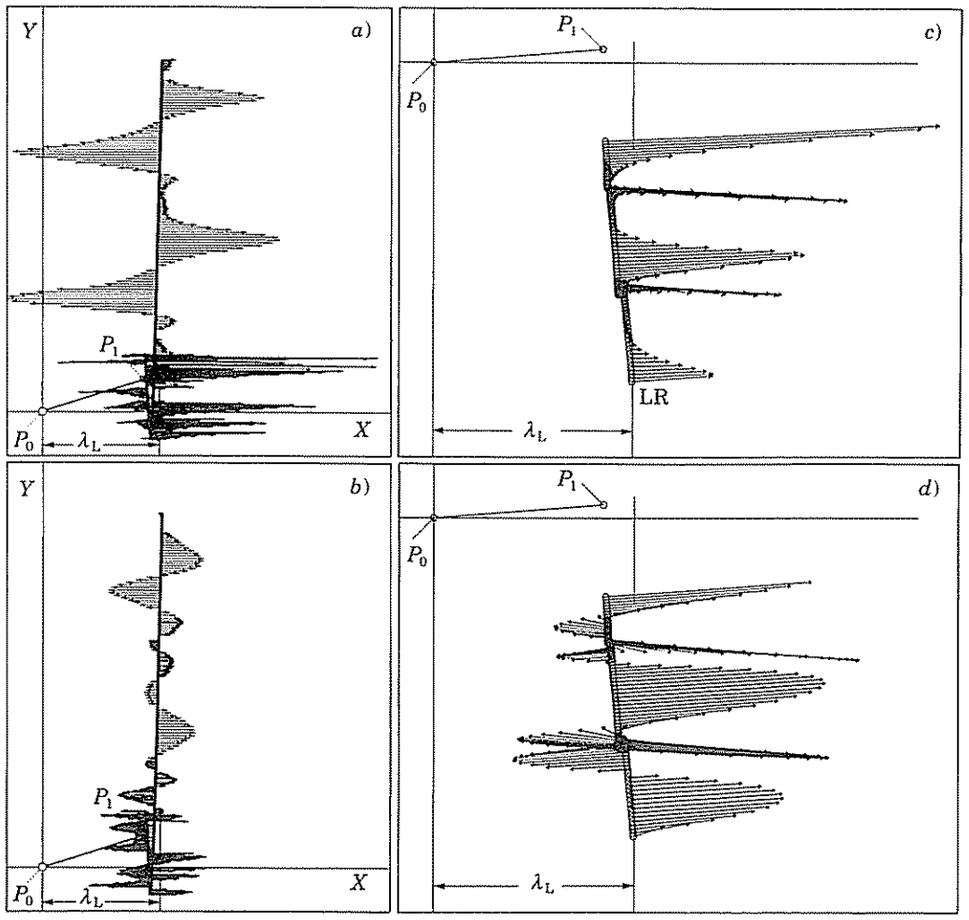

Fig. 6. – *a*) Force exerted on a single charge, initially placed at P_1, by a macrocharge of 10^8 electrons placed at P_0, being $\overline{P_0P_1}$ equal to $1\cdot10^{-3}$ cm. The kinetic energy of the charges is equal to 18 MeV. It is seen that the force, initially mainly in the forward direction, becomes basically symmetric when the bunching distance $\beta\lambda_L \simeq \lambda_L = 1.101\cdot10^{-3}$ cm is reached. The maximum wiggler magnetic field is taken to be $B_z = 5000$ G. The resonant-laser wave electric field is taken to be 1770 statvolt/cm. *b*) Force due to the resonant-laser fields acting on a single electron, initially in P_1, with the same parameters as in *a*). In the two cases the forces are represented in the same arbitrary units. *c*) Force exerted on a single charge by a macrocharge of 10^8 electrons. In this case the kinetic energy of the charges is equal to 7.48 MeV. The resonant-laser wave electric field is taken to be 10^4 statvolt/cm, a value too high used only for numerical simulation. *d*) Force due to the resonant-laser field acting on a single electron initially, in P_1, with the same parameters as in *c*).

with the wiggler field, which, as shown in fig. 6*a*) modulates the axial velocity of the electrons (phase bunching).

The force on a single electron due to the radiation fields of a macroparticle (which we assume here to be composed of a bunch of 10^8 electrons corresponding to a

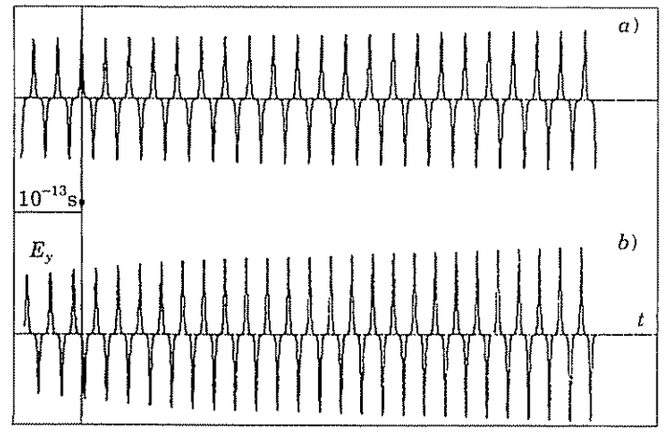

Fig. 7. – E_y-component of the radiation emitted by a single charge without perturbation of the other charges (*a*)) and taking account of the influence of the charges (10^8 electrons) of the following bunch (*b*)). E_y is represented in arbitrary units.

beam current of 450 A with the distance between bunches $\beta\lambda_L \cong 0.001$ cm) is shown in fig. 6*b*). These numerical examples are suggested by the FEL amplifier experiments carried out at Los Alamos National Laboratory using a high-power ((50 ÷ 900) MW)CO_2 laser and a r.f. linac [13], where, with an input laser signal of 750 MW (corresponding to an electric field of 1772.5 statvolt /cm for a laser beam cross-section of 1 cm^2), more than 50% of the electrons of the beam were found to be trapped by the ponderomotive wave and decelerated.

The details of the numerical code employed in the present paper are deferred

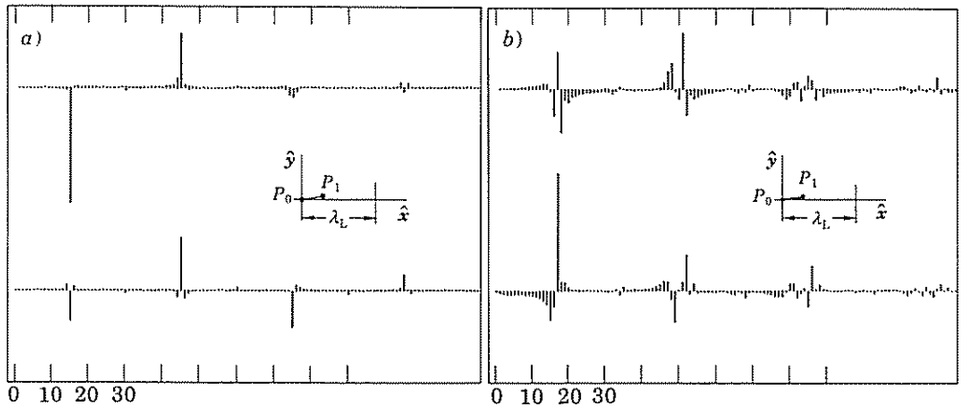

Fig. 8. – *a*) Spectral analysis of the radiation emitted by an unperturbed charge passing through a wiggler during the time of $5.4\cdot10^{-13}$ s. The particle is launched with a kinetic energy of 18.71 MeV into a wiggler with $\lambda_W = 2$ cm and $B_z = 5000$ G. *b*) The same for a charge perturbed by a macrocharge of 10^8 electrons placed at P_0. The distance $\overline{P_0P_1}$ is initially equal to $3\cdot10^{-4}$ cm.

to appendix A, while those of an alternative semi-numerical approach are given in appendix B.

In fig. 7 we represent the E_y component of the radiation emitted by a single charge both when perturbed by the presence of a second macrocharge (*b*)) and when such a second charge is absent (*a*)). The Fourier analysis of E_y (fig. 8) shows the effect of the perturbation due to a macrocharge of 10^8 electrons on a single electron at a distance less than $\lambda_L\beta$ (fig. 8*b*)). This diagram must be compared with that of an unperturbed electron (fig. 8*a*)).

5. – Conclusions.

In the current literature [9] the approach to FELs is based on a far-field approximation, where the fields, whose periodicity is dictated by the FEL geometry, is due to non-localized sources, and only the average velocity of moving charges is taken into consideration. Such an approach allows a description based on Fourier analysis, where all retardation effects in particle radiative interactions are neglected: any perturbation localized in time and space is therefore excluded, and no radiative instability may be taken into account. The near-field contributions are tentatively introduced, in ref. [6], for the one-electron off-axis radiation. The linear—undulator spectral brightness at a different observer/undulator distance is obtained from the S-Luce code that deals with a direct integration of the Lienard-Wiechert potential, and the electron trajectories are obtained from a Runge-Kutta integration. It must be noticed that, in this approach, no radiative interaction between charges is considered.

In the present paper, the electron interaction is numerically analysed by means of the relativistic (non-quantum) equations of motion and radiation. Our basic result consists in the Fourier analysis of the field emitted by a test charge moving in an FEL geometry. When the charge is not influenced by other particles of the beam, a normal ensemble of odd harmonics is seen, whose amplitude monotonously decreases with increasing frequency according to the value of the interaction strength a_W (fig. 8*a*)).

When, on the other hand, a perturbation due to another particle of the beam is taken into account (in the considered case a macrocharge of 10^8 electrons has been placed at a distance less than λ_L from the test charge) many supplementary harmonics and a considerable broadening of spectral lines is evidenced by numerical analysis (fig. 8*b*)).

The radiation emitted by a single charge shows in a simple way the distortion of the wave front outside the direction of the average particle motion. The main conclusion is that, when high-current densities are employed for the electron beam and high-radiation powers are injected along the beam, both instabilities and non-linear features make it difficult to classify the FELs as real lasers. Both the beam coherence and its collimation, in fact, diverge significantly from the conditions usually indicating a laser mechanism: the emitted radiation in particular is appreciably coherent only in a very narrow solid angle around the beam axis. This behaviour was also evidenced in ref. [14-16] in low-density relativistic electron beam when transverse spatial inhomogeneities in the wiggler field bring to a chaotic electron motion.

Devices able to generate electromagnetic-radiation beams with a low-divergence

angle and endowed with a high degree of coherence shall probably require new technological solutions, typically based on sophisticated systems of wave guides.

* * *

Thanks are due to Prof. C. Belli (Politecnico di Milano) for helpful discussions, and to Prof. A. Orefice (Università di Milano) for his fundamental help during the genesis of the work.

APPENDIX A

Numerical method.

The numerical computation of electron trajectories is performed by calculating the values of electric and magnetic fields at the beginning of each step and keeping them constant along it.

We chose the well-known Boris mover method [17, 18] modifying it in such a way to partition the electron orbits in acceptably small arcs of different lengths. The advancement step along the trajectories is fractioned in such a way to determine with any wanted approximation, the point where an electromagnetic signal emitted by a particle reaches the other one (see fig. 10). We shall call here «concurrence point» the position, along a particle trajectory, reached at time t by the radiation emitted by the other particle at the time $t - R/c$.

In the numerical computation of both particle trajectories we take into account, during the step preceding the first concurrence point, the only action of the wiggler field and of a possible externally injected resonant radiation.

Successively, of course, the full radiative-particle interaction is taken into consideration.

The information needed to start the numerical integration consists of the initial particle momentum and position.

In the usual application of the Boris method the two first-order differential relativistic equations, to be integrated separately for each particle, are eqs. (2.1) and (2.2).

By the substitution

$$\underline{u} = \underline{p}/m\,, \tag{A.1}$$

these equations are replaced by the finite-difference equations for $\underline{u}^{n+1/2}$

$$\frac{\underline{u}^{n+1/2} - \underline{u}^{n-1/2}}{\Delta t} = \frac{e}{m}\left[\underline{E}^n + \frac{(\underline{u}^{n+1/2} + \underline{u}^{n-1/2})}{2c\gamma^n} \times \underline{B}^n\right]. \tag{A.2}$$

The particle position vector $\underline{X}$ at the $(n+1)$-th step is obtained from the n-th one according to

$$\underline{X}^{n+1} = \underline{X}^n + \underline{v}^{n+1/2} \cdot \Delta t = \underline{X}^n + \frac{\underline{u}^{n+1/2} \cdot \Delta t}{\gamma^{n+1/2}}\,, \tag{A.3}$$

where $\gamma^{n+1/2} = [1 + (\underline{u}^{n+1/2}/c)^2]^{1/2}$.

This step produces a second-order error with respect to Δ/t in the particle orbit.

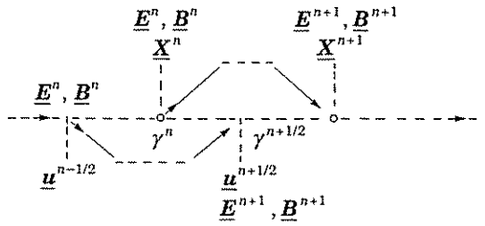

Fig. 9.

The numerical time advancement procedure is shown in fig. 9, together with the time centring. The initial conditions must be transformed, as a first step, to fit the numerical flow: this is obtained by pushing $\underline{u}(0)$ back to $\underline{u}(-\Delta t/2)$, using he force $\underline{F}$ calculated at $t = 0$ and $\underline{X}(0)$.

The usual Boris method [17,18] separates the electric and magnetic forces introducing into (A.2) the substitutions:

$$\underline{u}^{n-1/2} = \underline{u}^- - e\underline{E}^n \Delta t/2m , \tag{A.4}$$

$$\underline{u}^{n+1/2} = \underline{u}^+ + e\underline{E}^n \Delta t/2m . \tag{A.5}$$

It can then be seen that $\underline{E}^n$ cancels entirely, leaving

$$\frac{\underline{u}^+ - \underline{u}^-}{\Delta t} = \frac{e}{2mc\gamma^n}(\underline{u}^+ + \underline{u}^-) \times \underline{B}^n . \tag{A.6}$$

Equation (A.6) represents a rotation, around an axis parallel to $\underline{B}$, of the vector $\underline{u}^-$ into the vector $\underline{u}^+$ (having the same amplitude) by an angle

$$\theta = -2\,\mathrm{tg}^{-1}\left(\frac{eB\,\Delta t}{2mc\gamma}\right).$$

The magnetic field does not modify the amplitudes $|\underline{u}^-| = |\underline{u}^+| = |\underline{u}^n|$. The quantity γ^n is then obtained by the relation

$$\gamma^n = [1 + (u^-/c)^2]^{1/2} .$$

The approach of the present paper is, however, somewhat different from the aforementioned Boris method. It consists, in fact, in simplifying step by step the procedure of motion initialization, by replacing eq. (A.2) with the following modified difference equation:

$$\frac{\underline{u}^{n+\varepsilon} - \underline{u}^n}{\varepsilon\,\Delta t} = \frac{e}{m}\left[\underline{E}^n + \frac{(\underline{u}^{n+\varepsilon} + \underline{u}^n)}{2c\gamma^{n+\varepsilon/2}} \times \underline{B}^n\right] \tag{A.7}$$

and using a space increment given by

$$\underline{X}^{n+2\varepsilon} = \underline{X}^n + \frac{\underline{u}^{n+\varepsilon}\,\Delta t \cdot 2\varepsilon}{\gamma^{n+\varepsilon}}, \tag{A.8}$$

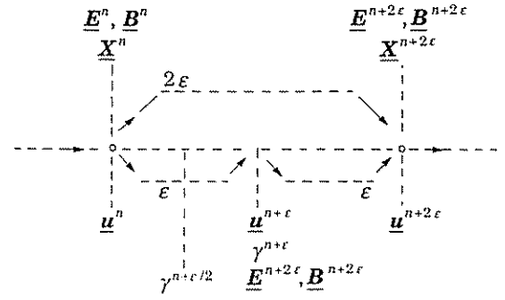

Fig. 10.

where ε ($\leqslant 1/2$) is a parameter, which must be recalculated at each step by a trial and error procedure (fig. 10).

For the separation of electric and magnetic field the following modified substitutions are employed:

$$\underline{u}^n = \underline{u}^- - e\underline{E}^n \varepsilon\,\Delta t/2m , \tag{A.9}$$

$$\underline{u}^{n+\varepsilon} = \underline{u}^+ + e\underline{E}^n \varepsilon\,\Delta t/2m , \tag{A.10}$$

which lead, using (A.7), to the basic equation

$$\frac{\underline{u}^+ - \underline{u}^-}{\varepsilon\,\Delta t} = \frac{e}{2mc\gamma^{n+\varepsilon/2}}(\underline{u}^+ + \underline{u}^-) \times \underline{B}^n . \tag{A.11}$$

The numerical steps of the present modified Boris method may be schematized as follows:

1) add half of the electric contribution to $\underline{u}^n$ using (A.9) to obtain $\underline{u}^-$ (having the same amplitude as $u^{n+\varepsilon/2}$) thus bringing to

$$\gamma^{n+\varepsilon/2} = [1 + (u^-/c)^2]^{1/2} ;$$

2) obtain $\underline{u}^+$ by the rotation (A.6), in the following way:

a) compute

$$\underline{u}' = \underline{u}^- + \underline{u}^- \times \underline{h} , \tag{A.12}$$

where

$$\underline{h} = \frac{e\underline{B} \cdot \varepsilon\,\Delta t}{mc2\gamma^{n+\varepsilon/2}} , \tag{A.13}$$

b) thus obtaining

$$\underline{u}^+ = \underline{u}^- + \underline{u}' \times \underline{s} , \tag{A.14}$$

where the vector $\underline{s}$ is parallel to $\underline{B}^n$ and its magnitude is determined by the

requirement $|\underline{u}^-| = |\underline{u}^+|$ so that

$$\underline{s} = 2 \cdot \underline{h}/(1 + h^2)\,; \tag{A.15}$$

3) add to $\underline{u}^+$ the remaining half of the electric contribution, using eq. (A.10); obtain $\underline{u}^{n+\varepsilon}$, and recalculate

$$\gamma^{n+\varepsilon} = [1 + (u^{n+\varepsilon}/c)^2]^{1/2}\,;$$

4) obtain the new position $\underline{X}^{n+\varepsilon}$ by means of (A.8).

The vector $\underline{u}$ is brought to the same time step of $\underline{X}^{n+2\varepsilon}$ by an increment $\varepsilon\,\Delta t$ given to $\underline{u}^{n+\varepsilon}$. The computation cycle may now be repeated until the requested orbit is entirely traced.

The time lag between position and momentum, required by any leap-frog method, is obtained by a space advancement corresponding to twice the time step $\varepsilon\,\Delta t$ employed to compute the particle momentum (fig. 10).

Each step requires of course the computation (to be performed by finding ε by trial and error) of the new concurrence point. At the beginning of each step, $\underline{X}$ and $\underline{u}$ are computed at the same time; then the increment of $\underline{u}^n$ is computed by a time step $\varepsilon\,\Delta t$, thus obntaining $\underline{u}^{n+\varepsilon}$ and giving the condition for the space advancement $\underline{X}^n \rightarrow \underline{X}^{n+2\varepsilon}$. If now $\underline{X}^{n+2\varepsilon}$ is found to satisfy the concurrence point conditions, the quantity $\underline{u}^{n+\varepsilon}$ is updated to $\underline{u}^{n+2\varepsilon}$, and the cycle may be repeated.

APPENDIX B

Analytical-numerical method.

The problem numerically solved in appendix A, may be faced by an alternative semi-analytical approach, based on the expression of the particle trajectory in constant electric and magnetic fields (fig. 11)[19,20], by means of a sequence of suitable changes of the reference frame.

Let L be the laboratory reference frame, where both $\underline{E}$ and $\underline{B}$ have arbitrary directions. A rotation is performed from L to frame K where the only non-zero field

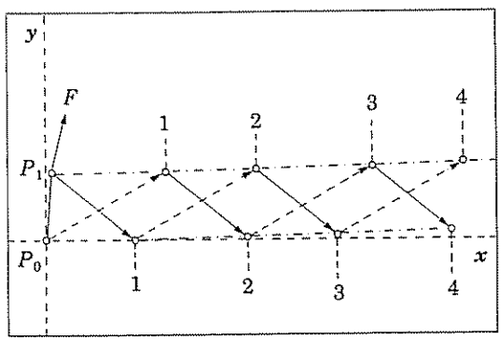

Fig. 11. – Trajectories of the two interacting particles. The numbers indicate the successive concurrent positions where the radiation coming from the retarded position of a particle hits another one. The particles are launched with a kinetic energy of 0.7477 MeV into a wiggler with $\lambda_W = 2\,\mathrm{cm}$ and $B_z = 10^5$ gauss. The initial distance $\overline{P_0P_1}$ is equal to $2 \cdot 10^{-4}\,\mathrm{cm}$.

components are E_{2k}, E_{3k}, B_{3k}. Then we pass from K to moving system K' where the electric and magnetic fields turn out to be parallel, with components E_2', E_3', B_2', B_3'. This is obtained by imposing that

$$\beta_K^2 - \beta_K(E_{2K}^2 + E_{3K}^2 + B_{3K}^2)/(E_{2K}B_{3K}) + 1 = 0\,, \qquad \gamma_K = (1 - \beta_K^2)^{-1/2}\,,$$

where $\beta_K c$ is the velocity of K' relative to K. Another rotation is now performed from K' to a system K'' where the electric and magnetics fields are parallel to the $\tilde{z}''$-axis.

The motion equations in K'' are given by [9]

$$\dot{P}_x'' = \Omega_0 P''(2)/\gamma''\,, \quad \dot{P}_y'' = -\Omega_0 P''(1)/\gamma''\,, \quad \dot{P}_z'' = eE_3''\,. \tag{B.1}$$

The trajectory equations in K'', obtained from (B.1), may be written in the form

$$\begin{cases} X''(t'') = [P_{0x}'' \sin\Phi - P_{0y}''(\cos\Phi - 1)]/\Omega_0 m\,, \\ Y''(t'') = [P_{0x}''(\cos\Phi - 1) + P_{0y}'' \sin\Phi]/\Omega_0 m\,, \\ Z''(t'') = mc^2\gamma_0[k\sqrt{1 + \tau^2(t'')} - 1]/eE_3''\,, \end{cases} \tag{B.2}$$

where $\underline{P}_0''$ is the initial particle momentum in the system K'',

$$\Phi(\tau) = B_3''(\sinh^{-1}\tau - \sinh^{-1}\tau_0)/E_3''\,,$$

$$\tau_0 = \varrho_{03}/m\gamma_0 ck\,, \quad \tau(t'') = (eE_3''t'' + \varrho_{03})/m\gamma_0 ck\,,$$

$$\gamma_0'' = \gamma''(P_0'')\,, \quad \varrho_{03} = P_0''(3)/mc\gamma_0\,, \quad \Omega_0 = eB_3''/mc\,, \quad K = (1 - \varrho_{03}^2)^{1/2}\,,$$

$$\gamma'' = \left[1 + \left(\frac{P''}{mc}\right)^2\right]^{1/2}\,, \quad P''^2 = P_x''^2 + P_y''^2 + P_z''^2\,,$$

and t'' is the proper time in the system K'' (and therefore in K'). We may express the momentum components in the form

$$P_x'' = P_{0x}'' \cos\Phi\,, \quad P_y'' = -P_{0y}'' \sin\Phi\,, \quad P_z'' = eE_3''t'' + P_{0z}''\,. \tag{B.3}$$

The particle coordinates and momentum components have now to be transformed back to the laboratory frame L. The transformation from K'' to K' is determined by a back-rotation by an angle $-\theta$:

$$X' = X''\,, \quad Y' = Y''\cos\theta + Z''\sin\theta\,, \quad Z' = -Y''\sin\theta + Z''\cos\theta\,.$$

We pass now from K' to K by the relativistic transformations

$$\begin{cases} X_K(t'') = \gamma_K[X'(t'') + \beta_K t'' c]\,, \quad Y_K(t'') = Y'(t'')\,, \quad Z_K(t'') = Z'(t'')\,, \\ t_K(t'') = \gamma_K[t'' + \beta_K X_K(t'')/c]\,, \quad (t_K \equiv t_L)\,, \\ P_{Kx} = \gamma_K[P_x' + E_t'\beta_K/c]\,, \quad P_{Ky} = P_y'\,, \quad P_{Kz} = P_z'\,, \end{cases} \tag{B.4}$$

where $E_t' = mc^2\gamma''$ is the particle energy both in K' and K''.

Finally, the passage from K to L is obtained by means of a rotation opposite to the one performed from L to K. When all the quantities describing the particle motion in

the laboratory system L turn out, by means of a numerical procedure analogous to that described in appendix A, to satisfy the concurrence point conditions, the analytical-numerical cycle may be repeated by computing the new quantities with the updated values of the fields and by assuming the value of the last particle momentum value $\underline{P}_L$ as the starting one $\underline{P}_{0L}$ of the new cycle. The resulting orbits of the two interacting electrons are shown in fig. 11.

The semi-analytical method described in the present appendix B becomes competitive when the variation length of the external fields is large enough, and when the relative influence of the radiated fields is small enough (Compton regime), to allow long steps in the numerical computation. In the typical cases treated in the present paper the two approaches turn out to be almost equivalent.

REFERENCES

[1] B. PODOLSKY and K. S. KUNZ: *Fundamentals of Electrodynamics* (Marcel Dekker, New York and London, 1969).
[2] C. G. DARWIN: *Philos. Mag.*, 39, 537 (1920); G. BREIT: *Phys. Rev.*, 39, 616 (1932).
[3] J. D. JACKSON: *Classical Electrodynamics* (John Wiley, New York, NY, 1975).
[4] R. A. MOORE, T. C. SCOTT and M. B. MORGAN: *Phys. Rev. Lett.*, 59, 525 (1987); *Can. J. Phys.*, 66, 206 (1988); R. A. MOORE and T. C. SCOTT: *Can. J. Phys.*, 66, 365 (1988).
[5] R. N. HILL: *J. Math. Phys.*, 8, 201 (1967).
[6] R. BARBINI *et al.*: *Riv. Nuovo Cimento*, 13, No. 6 (1990).
[7] P. LUCHINI and H. MOTZ: *Undulators and Free-Electron Lasers* (Oxford University Press, Oxford, New York, Toronto, 1990).
[8] B. D. MCVEY: *Nucl. Instrum. Methods A*, 250, 449 (1986).
[9] T. M. TRAN and J. S. WURTELE: *Review of Free-Electron-Laser (FEL) Simulation Techniques*, CRPP-LRP392/90 (Ecole Polytechnique Federale de Lusanne - Suisse, 1990).
[10] L. LANDAU and E. LIFCHITZ: *Theorie du champ* (MIR, Moscow, 1966).
[11] A. AMIR *et al.*: *Cylindrical Gaussian eigenmodes of a rectangular waveguide resonator, three-dimensional numerical calculations of gain per mode*, in *Free-Electron Generators of Coherent Radiation*, edited by C. A. BRAU *et al.*, SPIE, 453 (SPIE, Bellingham, WA, 1984).
[12] A. GOVER. A. FRIEDMAN and A. LUCCIO: *Nucl. Intrum. Methods A*, 259, 163 (1987).
[13] R. W. WARREN *et al.*: *IEEE J. Quantum Electron.*, QE-19, 391 (1983).
[14] C. CHEN and R. C. DAVIDSON: *Phys. Rev. A*, 42, 5041 (1990).
[15] C. CHEN and R. C. DAVIDSON: *Chaotic Particle Dynamics in Free Electron Lasers*, PFC/JA-90-10 (1990) (Plasma Fusion Center, MIT, Cambridge, MA 02139).
[16] C. CHEN and R. C. DAVIDSON: *Phys. Fluids B*, 2, 171 (1990).
[17] J. P. BORIS: *Relativistic plasma simulation*, in *Proceedings of the Fourth Conference on Numerical Simulation of Plasmas*, edited by J. BORIS and R. SHANNY (NRL, Washington, D.C., 1970), p. 3.
[18] C. K. BIRDSALL, A. BRUCE and I. LONGDON: *Plasma Physics Via Computer Simulation* (McGraw-Hill, New York, NY, 1985).
[19] R. GIOVANELLI: *Nuovo Cimento, D*, 9, 1443 (1987).
[20] JU. V. NOVOŽILOV and JU. A. JAPPA: *Elettrodinamica* (MIR, Moscow, 1987).